

Project Title: Chill Down Process of Hydrogen Transport Pipelines

Task PI: Renwei Mei, Department of Mechanical and Aerospace Engineering
Co-I: James Klausner, Department of Mechanical and Aerospace Engineering

Project Goals

The objective of this research task is to experimentally and computationally study the unsteady dynamics of a liquid hydrogen wave front translating down a pipeline during the chill down mode and develop a comprehensive computational model to predict the associated flow fields, thermal fields, and residence time. In order to accomplish the objective, the following tasks are planned: a) experimentally study the dynamics of a propagating liquid hydrogen wave front, b) experimentally measure the heat transfer rate associated with film boiling beneath the wave front, c) experimentally investigate transient nucleate boiling heat transfer associated with liquid film flow, d) develop a comprehensive computational model to predict the flow and temperature fields associated with propagating liquid hydrogen waves, and e) develop engineering models for cryogenic practitioners to predict the required chill down residence time under a variety of different operating conditions.

Accomplishments

Abstract

A pseudo-steady model has been developed to predict the chilldown history of pipe wall temperature in the horizontal transport pipeline for cryogenic fluids. A new film boiling heat transfer model is developed by incorporating the stratified flow structure for cryogenic chilldown. A modified nucleate boiling heat transfer correlation for cryogenic chilldown process inside a horizontal pipe is proposed. The efficacy of the correlations is assessed by comparing the model predictions with measured values of wall temperature in several azimuthal positions in a well controlled experiment by Chung et al. (2004). The computed pipe wall temperature histories match well with the measured results. The present model captures important features of thermal interaction between the pipe wall and the cryogenic fluid, provides a simple and robust platform for predicting pipe wall chilldown history in long horizontal pipe at relatively low computational cost, and builds a foundation to incorporate the two-phase hydrodynamic interaction in the chilldown process.

Introduction

The cryogenic chilldown is encountered in many applications but is of particular importance in cryogenic transportation pipelines. For example, in rockets or space shuttle launch facility, cryogenic liquids as fuel are filled from the storage tank to the internal fuel tanks of a space vehicle through a complex pipeline system. To avoid evaporated fuel entering the space vehicle, a cryogenic chilldown prior to the filling is required to reduce the pipe wall temperature to the saturation temperature of the cryogenic liquid.

Cryogenic chilldown involves complicated hydrodynamic and thermal interactions among liquid, vapor, and solid pipe wall. There exist few basic experimental studies and modeling efforts for chilldown of cryogenic fluids. Studies on cryogenic chilldown started in 1960's accompanying the development of rocket launching system. Early experimental studies were conducted by Burke et al. (ref. 1), Graham (ref. 2), Bronson et al. (ref. 3), Chi and Vetere (ref. 4), Steward (ref. 5) among other researches. Bronson et al. (ref. 3) studied the flow regime in a horizontal pipe during the chilldown by liquid hydrogen. The results revealed that the stratified flow is prevalent in the cryogenic chilldown.

Flow regimes and heat transfer regimes in the horizontal pipe chilldown were also studied by Chi and Vetere (ref. 4). Information of flow regimes was deduced by studying the fluid temperature and volume fraction during the chilldown. Several flow regimes were identified: single phase vapor, mist flow, slug flow, annular flow, bubbly flow, and single-phase liquid flow. Heat transfer regimes were identified as: single-phase vapor convection, film boiling, nucleate boiling, and single-phase liquid convection.

Recently, Velat et al. (ref. 6) systematically studied cryogenic chilldown in a horizontal pipe. Their study included: visually recording the chilldown in a transparent Pyrex pipe, which is used to identify the flow regime and heat transfer regime; collecting temperature histories at different positions of wall in the chilldown; recording pressure drop along the pipe. Chung et al. (ref. 7) conducted a similar study on the nitrogen chilldown at relatively low mass flux and provided the data needed to assess various heat transfer coefficients in the present study.

Burke et al. (ref. 1) developed a crude chilldown model based on the 1-D heat transfer through the pipe wall and the assumption of infinite heat transfer rate from the cryogenic fluid to the pipe wall. The effects of flow regimes on the heat transfer rate were neglected. Graham et al. (ref. 2) correlated heat transfer coefficient and pressure drop with the Martinelli number (ref. 8) based on their experimental data. Chi (ref. 9) developed a 1-D model for energy equations of the liquid and the wall, based on film boiling heat transfer between the wall and fluid. An empirical equation for predicting chilldown time and temperature was proposed.

Steward (ref. 5) developed a homogeneous flow model for the chilldown. The model treated the cryogenic fluid as a homogeneous mixture. The continuity, momentum and energy equations of mixture were solved to obtain density, pressure and temperature of mixture. Various heat transfer regimes were considered: film boiling, nucleate boiling and single-phase convection heat transfer. Separate treatment of different heat transfer regimes resulted in a significant improvement in the prediction of the chilldown process. Homogeneous mixture model was also employed by Cross et al. (ref. 10) who obtained a correlation for the wall temperature in the chilldown with an oversimplified heat transfer model of the heat transfer between the wall and the fluid.

Stratified flow regime, which is the prevalent flow regime in horizontal chilldown, was first studied by Chen and Banerjee (refs. 11 to 13). They developed a separated flow model for the simulating cool-down by a stratified flow in a hot horizontal pipe. Both phases were modeled using 1-D mass and momentum conservation equations. The wall temperature was computed using a 2-D transient heat conduction equation. Their prediction for wall temperature agreed well with their experimental results. Although a significant progress was made on handling the momentum equations, the heat transfer correlations employed were not as advanced.

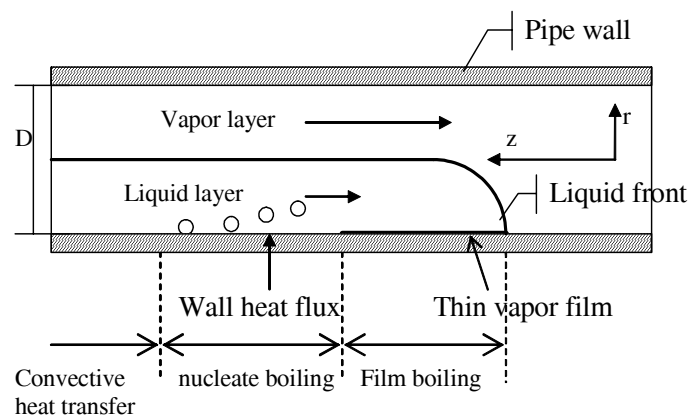


Figure 1.—Schematic of chilldown heat transfer regimes in a horizontal pipe.

Typical chilldown involves several heat transfer regimes as shown in figure 1. Near the liquid front is the film boiling. The knowledge of the heat transfer in the film boiling regime is relatively limited, because i) film boiling has not been the central interest in industrial applications; and ii) high temperature difference causes the difficulties in experimental investigations. For the film boiling on vertical surfaces, early work was reported by Bromley (ref. 14), Dougall and Rohsenow (ref. 15) and Lavery and Rohsenow (ref. 16). Film boiling in a horizontal cylinder was first studied by Bromley (ref. 17); and the Bromley correlation was widely used. Breen and Westwater (ref. 18) modified Bromley's equation to account for very small tubes and large tubes. If the tube is larger than wavelength associated with the Taylor instability, the heat transfer correlation is reduced to Berenson's correlation (ref. 19) for a horizontal surface.

Empirical correlations for film boiling were proposed by Hendrick et al. (refs. 20 and 21), Ellerbrock et al. (ref. 22), von Glahn (ref. 23), Giarratano and Smith (ref. 24). These correlations relate a simple or modified Nusselt number ratio to the Martinelli parameter. Giarratano and Smith (ref. 24) gave detailed assessment on these correlations. All these correlations are for steady state cryogenic film boiling. They may not be suited for transient chilldown application.

When the pipe chills down further, film boiling ceases and transient boiling occurs, followed by nucleate boiling. The heat transfer in the transient boiling is even more complicated and it is usually assumed that the boiling switches from film boiling to nucleate boiling right away. The position of film boiling transitioning to the nucleate boiling is often called rewetting front, because from that position the cold liquid starts touching the pipe wall. Usually the Leidenfrost temperature indicates the transition from the film boiling to the nucleate boiling.

The study on the convection nucleate boiling is extensive. A general correlation for saturated boiling was introduced by Chen (ref. 25). Gungor and Winterton (ref. 26) modified Chen's correlation and extend it to subcooled boiling. Enhancement and suppression factors for macro-convective heat transfer were introduced. Gungor and Winterton's correlation can fit experimental data better than the modified Chen's correlation (ref. 27) and Stephan and Auracher correlation (ref. 28). Kutateladze (ref. 29) and Steiner (ref. 30) also provided correlations for cryogenic fluids in pool boiling and forced convection boiling. Although they are not widely used, they should be more applicable for cryogenic fluids as the correlation was directly based on cryogenic conditions.

As the wall temperature drops further, the nucleate boiling is replaced by pure convection. The convection heat transfer can be modeled using Dittus-Boelter equation (ref. 31) for the fully developed turbulent pipe flow or corresponding laminar heat transfer equation for laminar pipe flow (ref. 31). The condition in which nucleate boiling switches to single-phase convection heat transfer is that all nucleate sites are suppressed.

Although two-fluid model can describe the fluid dynamics aspect of the chilldown process, it suffers from computational instability for moderately values of slip velocity between two phases which limits its application. To gain fundamental insight into the thermal interaction between the wall and the cryogenic fluid and to be able to rapidly predict chilldown in a long pipe, an alternative pseudo-steady model is developed. In this model, liquid wave front speed is assumed to be constant and is the same as the bulk liquid speed (ref. 32). It is also assumed that steady state thermal fields for both the liquid and the solid exist in a reference frame that is moving with the wave front. The heat transfer between the fluid and the wall is modeled using different heat transfer correlations depending on the operating heat transfer regime at a given location. Various improvements on the correlations are introduced, including the development of a new film boiling heat transfer coefficient. The governing equation for the solid thermal field becomes a parabolic equation that can be efficiently solved. It must be emphasized that a great advantage of the pseudo-steady model is that one can assess the efficacy of the film boiling model independently from that of the nucleate boiling model since the down stream information in the nucleate boiling regime cannot affect the temperature in the film boiling regime. In another word, even if the nucleate boiling heat transfer coefficient is inadequate, the film boiling heat transfer coefficient can still be assessed in the film boiling regime by comparing with the measure temperature for the right period of time. After the satisfactory performance is achieved for the film boiling regime, the nucleate boiling heat transfer model

can be subsequently assessed. In the Results section, those detailed assessments of the heat transfer coefficients are provided by comparing the computed temperature variations with the experimental measurements of Chung et al. (ref. 7). Satisfactory results are obtained.

Nomenclature

Bo	Boiling number
c	solid heat capacity
c_p	heat capacity
D	pipe diameter
d	thickness of pipe wall
g	gravity
h	heat transfer coefficient
h_{pool}	pool boiling heat transfer coefficient
h_{conv}	convection boiling heat transfer coefficient
h_{fg}	latent heat
Ja	Jacob number
k	thermal conductivity
k_{eff}	effective thermal conductivity
Nu	Nusselt number
p	pressure
R	radius of pipe
R_1 and R_2	inner and outer radius of pipe
Ra	Rayleigh number
Re	Reynolds number
Pc	Peclet number
Pr	Prandtl number
S	suppression factor
T	temperature
T_1	Leidenfrost temperature
T_2	transition temperature between nucleate boiling to convection heat transfer
T_o	room temperature
t	time
U	velocity
u and v	vapor film velocity
x and y	vapor film coordinates
Z	transformed coordinate
$z, r,$ and ϕ	cylindrical coordinates
α	liquid volume fraction
χ_{tt}	Martinelli number
δ	vapor film thickness
ε	emissivity
ϕ	azimuthal coordinate
μ	viscosity
θ	dimensionless temperature; azimuthal coordinate
σ	liquid surface tension; Stefan Boltzmann constant

Subscripts

0	characteristic value
i and o	inner and outer pipe

<i>l</i>	liquid
<i>v</i>	vapor
<i>w</i>	wall
sat	saturated

Superscripts

' dimensionless variable

Formulation

In pseudo-steady chilldown model, it is assumed that both the liquid and its wave front moves at a constant speed *U* which is taken from estimated experimental condition in the present model. Thus the main emphasis of the present study is on the modeling of the heat transfer coefficients in different heat transfer regimes and the computation of the thermal field within the solid pipe.

Solid Heat Transfer

The thermal field inside the solid wall is governed by the 3-D unsteady energy equation:

$$\rho c \frac{\partial T}{\partial t} = \frac{\partial}{\partial z} \left(k \frac{\partial T}{\partial z} \right) + \frac{1}{r} \frac{\partial}{\partial r} \left(r k \frac{\partial T}{\partial r} \right) + \frac{1}{r} \frac{\partial}{\partial \phi} \left(\frac{k}{r} \frac{\partial T}{\partial \phi} \right) \tag{1}$$

Since the wave front speed *U* is assumed to be a constant, it can be expected that when the front is reasonably far from the entrance region of the pipe, the thermal field in the solid is in a steady state when it is viewed in the reference frame that moves with the wave front. Thus, the following coordinate transformation is introduced,

$$Z = z + Ut . \tag{2}$$

Equation (1) is then transformed to:

$$\rho c U \frac{\partial T}{\partial Z} = \frac{\partial}{\partial Z} \left(k \frac{\partial T}{\partial Z} \right) + \frac{1}{r} \frac{\partial}{\partial r} \left(r k \frac{\partial T}{\partial r} \right) + \frac{1}{r} \frac{\partial}{\partial \phi} \left(\frac{k}{r} \frac{\partial T}{\partial \phi} \right) . \tag{3}$$

For further simplification, the following dimensionless parameters are introduced,

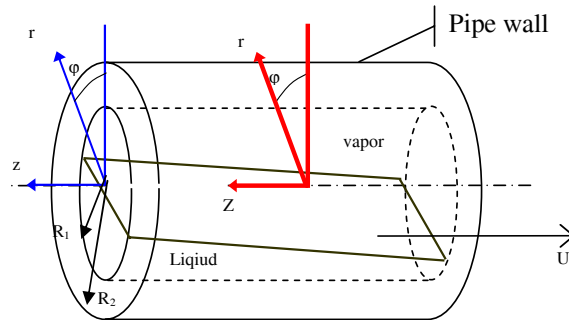


Figure 2.—Coordinate systems: laboratory frame is denoted by *z*, moving frame is denoted by *Z*.

$$\theta = \frac{T - T_w}{T_w - T_{sat}}, \quad Z' = \frac{Z}{d}, \quad r' = \frac{r}{d} \quad c' = \frac{c}{c_0} \quad \text{and} \quad k' = \frac{k}{k_0} \quad (4)$$

where k_0 is the characteristic thermal conductivity, and c_0 is the characteristic heat capacity. Equation (3) can be normalized as

$$Pc * c' \frac{\partial \theta}{\partial Z'} = \frac{\partial}{\partial Z'} \left(k' \frac{\partial \theta}{\partial Z'} \right) + \frac{1}{r'} \frac{\partial}{\partial r'} \left(r' k' \frac{\partial \theta}{\partial r'} \right) + \frac{1}{r'} \frac{\partial}{\partial \phi} \left(\frac{k'}{r'} \frac{\partial \theta}{\partial \phi} \right), \quad (5)$$

where $Pc = \frac{\rho c_0 U d}{k_0}$ is the Peclet number.

Under typical operating condition for the cryogenic chilldown process, $Pc \sim O(10^2) - O(10^3)$. The first term on the RHS of eq. (5) is small compared with the rest of terms and thus can be neglected. eq. (5) becomes

$$Pc * c' \frac{\partial \theta}{\partial Z'} = \frac{1}{r'} \frac{\partial}{\partial r'} \left(r' k' \frac{\partial \theta}{\partial r'} \right) + \frac{1}{r'} \frac{\partial}{\partial \phi} \left(\frac{k'}{r'} \frac{\partial \theta}{\partial \phi} \right), \quad (6)$$

which is parabolic. Hence in the Z' -direction, only one condition is needed. In the ϕ -direction, periodic boundary conditions are used. On inner and outer surfaces of the pipe wall, where $r = R_1$ and R_2 , proper boundary conditions for the temperature are required.

For convenience, $Z' = 0$ is set at the liquid wave front. In the region of $Z' < 0$, the inner wall is exposed to the pure vapor. Although there may be some liquid droplets in the vapor that can cause evaporative cooling when the droplets deposit on the wall and the cold flowing vapor can absorb some heat from the wall, the heat flux due to these two mechanisms is small compared with the heat transfer between liquid and solid wall in the region of $Z' > 0$. Hence, heat transfer for $Z' < 0$ is neglected and it is assumed that $\theta = 1$ at $Z' = 0$. The computation starts from the $Z' = 0$ to $Z' \rightarrow \infty$, until a steady state solution in the Z' -direction is reached. An implicit scheme in the Z' -direction is employed to solve eq. (6).

Liquid and Vapor Flow

The two-phase flow is assumed to be stratified as was observed in (ref. 7). Both liquid and vapor phases are assumed to be at the saturated state. Liquid volume fraction determining which part of wall is in contact with the liquid or the vapor, is specified at every cross-section along the Z' -direction based on experimental information. The visual studies (refs. 6 and 7) show that the liquid volume fraction increases gradually, rather than abruptly, near the liquid wave front and becomes almost constant during most of the chilldown. Hence, the following liquid volume fraction α as a function of time is used in the computation of the solid-fluid heat transfer coefficient,

$$\alpha = \alpha_0 \sin \left(\frac{t}{t_0} \cdot \frac{\pi}{2} \right) \quad t < t_0, \quad (7)$$

$$\alpha = \alpha_0 \quad t \geq t_0$$

where t_0 is characteristic chilldown time, and α_0 is characteristic liquid volume fraction. Here the time when the nucleate boiling is almost suppressed and slope of the wall temperature profile becomes flat is set as characteristic chilldown time.

The vapor phase velocity is assumed to be a constant. However, it was not directly measured. It is computationally determined by trial-and-error by fitting the computed and measured wall temperature variations for numerous positions.

Heat Transfer Between Cryogenic Fluid and Solid Pipe Wall

During the chilldown, the fluid in contact with the pipe wall is either liquid or vapor. The mechanisms of heat transfer between the liquid and the wall and between the vapor and the wall are different. Based on experimental measurements and theoretical analysis, liquid-solid heat transfer accounts for a majority of the total heat transfer. However, the prediction for heat transfer is much more complicated than the heat transfer between the vapor and the wall. The heat transfer between the liquid and the wall is discussed first.

Heat Transfer Between Liquid and Solid wall

Heat transfer between liquid and solid wall includes film boiling, nucleate boiling, and single-phase convection heat transfer. The transition from one type of boiling to another depends on many parameters, such as wall temperature, wall heat flux, and various properties of fluid. For simplicity, a fixed temperature approach is adopted to determine the transition points. That is, if the wall temperature is higher than the Leidenfrost temperature, film boiling dominates. If the wall temperature is between Leidenfrost temperature and a transition temperature, T_2 , nucleate boiling takes place. Here, the transient boiling regime between film boiling and nucleate boiling is neglected. The reason is mainly the difficulty associated with the determination of the conditions for the transient boiling to occur and the lack of a reliable transient heat transfer correlation. If the wall temperature is below the transition temperature T_2 , pure convection heat transfer dominates. The values of Leidenfrost temperature and transition temperature are determined by matching model prediction with the experimental results.

Film boiling heat transfer.—Because of the nature of high wall superheat in chilldown, the film boiling plays a major role in chilldown in terms of the time span and in terms of the total amount of heat removed from the wall. Currently there exists no specific film boiling correlation for chilldown applications with such high superheat. If one uses conventional film boiling correlations, necessary modifications for cryogenic application must be made for chilldown.

One of cryogenic film boiling heat transfer correlations was provided by Giarratano and Smith (ref. 24)

$$\left(\frac{\text{Nu}}{\text{Nu}_{calc}} \right) * \text{Bo}^{-0.4} = f(\chi_{tt}) \quad (8)$$

where Nu_{calc} is the Nusselt number for the forced convection heat transfer. In this correlation, the heat transfer coefficient is the averaged value for the whole cross section. Similar correlations for cryogenic film boiling also exist in literature. The correlations were obtained from measurements conducted under steady states. The problem with the use of this steady state film boiling correlation is that it does not take into account the change of flow regime as encountered in the chilldown. For example, for the same quality, the heat transfer rate in annular flow is much different from that in stratified flow, while those empirical correlations cannot take such difference into account.

Furthermore, in this study, local heat transfer coefficient is needed in order to incorporate the thermal interaction with the pipe wall. Since the two-phase flow regime information is available through visualization in the present study, the modeling effort needs to take into account the knowledge of the flow regimes.

There are several correlations for the film boiling based on the analysis of vapor film boundary layer and stability of the thin vapor film, such as Bromley's correlation (ref. 17) and Breen and Westerwater's correlation (ref. 18) for film boiling on the outer surface of a hot tube, Frederking and Clark's (ref. 33) and Carey's (ref. 34) correlations for film boiling on the surface of a sphere. However, none of these was obtained for cryogenic fluids or for film boiling on the inner surface of a pipe.

A new correlation for the film boiling in cryogenic chilldown inside a tube is presented here. The schematic of film boiling inside a pipe is shown in figure 3 with a cross-sectional view. Bulk liquid is

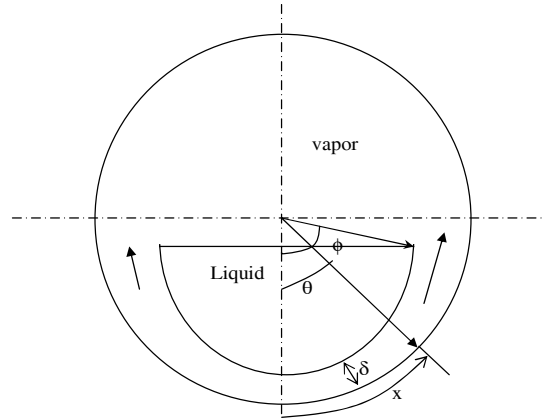


Figure 3.—Schematic diagram of film boiling in stratified flow.

near the bottom of the pipe. Beneath the liquid is a thin vapor film. Due to buoyancy force, the vapor in the film flows upward along the azimuthal direction. Heat is transferred through the thin vapor film from the solid to the liquid. Reliable heat transfer correlation for film boiling in pipes or tubes requires the knowledge of the thin vapor film thickness which can be obtained by solving the film layer continuity, momentum, and energy equations.

To simplify the analysis for the vapor film heat transfer, it is assumed the liquid velocity in the azimuthal direction is zero and the vapor flow in the direction perpendicular to the cross-section is negligible. It is further assumed that the vapor film thickness is small compared with the pipe radius and vapor flow is in steady state, incompressible and laminar. The laminar flow assumption can be confirmed *post priori* as the Reynolds number, Re , based on the film velocity and film thickness is typically of $O(10^0 \sim 10^0)$. In terms of the x - and y -coordinates and (u, v) velocity components shown in figure 3, the governing equations for the vapor flow are similar to boundary-layer equations:

$$\frac{\partial u}{\partial x} + \frac{\partial v}{\partial y} = 0, \quad (9)$$

$$u \frac{\partial u}{\partial x} + v \frac{\partial u}{\partial y} = -\frac{1}{\rho_v} \frac{\partial p}{\partial x} + \nu_v \frac{\partial^2 u}{\partial y^2} - g \sin \theta, \quad (10)$$

$$u \frac{\partial T}{\partial x} + v \frac{\partial T}{\partial y} = \alpha_v \frac{\partial^2 T}{\partial y^2}, \quad (11)$$

where subscript v refers to properties of vapor.

Because the length scale in the azimuthal (x) direction is much larger than the length scale at the normal (y) direction, the v -component may be neglected. Furthermore, the convection term is assumed small and is neglected. The resulting momentum equation is simplified to

$$\frac{1}{\rho_v} \frac{\partial p}{\partial x} = \nu_v \frac{\partial^2 u}{\partial y^2} - g \sin \theta. \quad (12)$$

The vapor pressure can be evaluated by considering the hydrostatic pressure from liquid core as:

$$p = p_0 + \rho_l g R \left(\cos\left(\frac{x}{R}\right) - \cos\phi \right) \quad (13)$$

where ϕ is angular position where the film merges with the vapor core. The momentum equation becomes

$$\frac{(\rho_l - \rho_v)}{\rho_v} g \sin\left(\frac{x}{R}\right) + \nu_v \frac{\partial^2 u}{\partial y^2} = 0. \quad (14)$$

The vapor velocity boundary condition is $u = 0$ at $y = 0$ and $u = u_l = 0$ at $y = \delta$. The vapor velocity profile is:

$$u = \frac{(\rho_l - \rho_v)}{2\nu_v \rho_v} g \sin\left(\frac{x}{R}\right) * (\delta y - y^2). \quad (15)$$

The mean velocity \bar{u} is

$$\bar{u} = \frac{1}{\delta} \int_0^\delta u dy = \frac{(\rho_l - \rho_v) \delta^2 g}{12\nu_v \rho_v} \sin\left(\frac{x}{R}\right). \quad (16)$$

The energy and mass balances on the vapor film requires that

$$\frac{k_v}{h_{fg}} dx * \left[-\left(\frac{\partial T}{\partial y}\right)_{y=\delta} \right] = \dot{m} = \rho_v d(\bar{u}\delta). \quad (17)$$

Neglecting the convection, the vapor energy equation is:

$$\frac{\partial^2 T}{\partial y^2} = 0. \quad (18)$$

The following linear temperature profile is thus obtained,

$$\frac{T - T_{sat}}{T_w - T_{sat}} = 1 - \frac{y}{\delta}. \quad (19)$$

Substituting the temperature and velocity profiles into eq. (17) yields

$$\frac{\delta}{R} \frac{d}{d\theta} \left(\left(\frac{\delta}{R} \right) \sin\theta \right) = \frac{12k_v \nu_v}{h_{fg} (\rho_l - \rho_v) g R^3} (T_w - T_{sat}). \quad (20)$$

Equation (20) has analytical solution:

$$\frac{\delta}{R} = 2 \left(\frac{6Ja}{Ra} \right)^{\frac{1}{4}} F(\theta), \quad (21)$$

where Ja is Jacob number and Ra is Raleigh number:

$$\text{Ja} = \frac{c_{p,v}(T_w - T_{sat})}{h_{fg}}, \quad (22)$$

$$\text{Ra} = \frac{gD^3(\rho_l - \rho_v)}{\nu_v \alpha_v \rho_v}, \quad (23)$$

and $F(\theta)$

$$F(\theta) = \left(\frac{\frac{4}{3} \int_0^\theta \sin^{1/3} \theta' d\theta'}{\sin^{4/3} \theta} \right)^{1/4} \quad (24)$$

describes the geometric dependence of vapor film thickness.

The mean velocity \bar{u} as a function of θ is thus

$$\bar{u} = \left(\frac{(T_w - T_{sat})(\rho_l - \rho_v)gR}{12\nu_v \rho_v^2 h_{fg}} \right)^{1/2} F^2(\theta) \sin(\theta). \quad (25)$$

Curves for $F(\theta)$ and $F^2(\theta)\sin \theta$ based on numerical integration are shown in figure 4. The vapor film thickness has a minimum at $\theta = 0$ and is nearly constant for $\theta < \pi/2$. It rapidly grows after $\theta > \pi/2$. The singularity at the top of tube when $\theta \rightarrow \pi$ is of no practical significance since the film will merge with the vapor core at the vapor-liquid interface. The vapor velocity is controlled by $F(\theta)^2 \sin \theta$ which is zero at the bottom of the pipe and increases almost linearly in the lower part of the tube where the vapor film

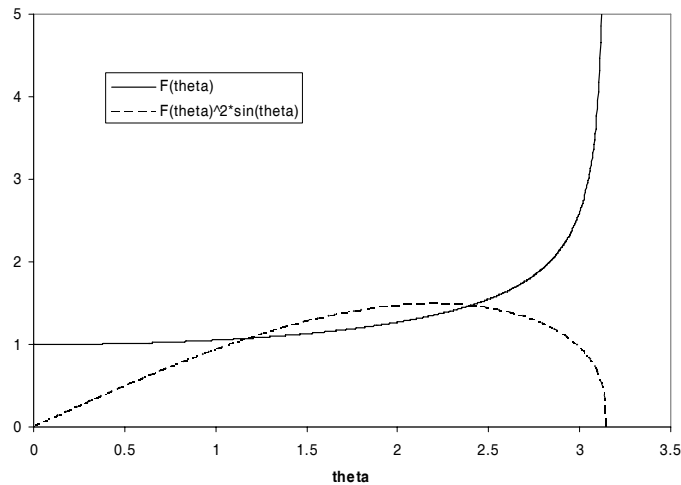


Figure 4.—Numerical solutions of the vapor thickness and velocity influence functions.

thickness does not change substantially. In the upper part of the tube, due to the increase in the vapor film thickness, the vapor velocity gradually drops back to zero at the top of the tube. Thus a maximum velocity may exist in the upper part of the tube.

The local film boiling heat transfer coefficient is easily obtained from the linear temperature profile. It is

$$h = \frac{k_v}{\delta} = 0.6389 \frac{k_v}{DF(\theta)} \left(\frac{Ra}{Ja} \right)^{\frac{1}{4}}. \quad (25)$$

Nucleate Boiling and Convection Heat Transfer

For the nucleate flow boiling heat transfer, Gungor and Winterton's correlation (ref. 26) is widely used due to its relatively better accuracy in predicting heat transfer coefficients. However, a closer examination on this correlation shows that it is based mainly on the following parameters: Pr, Re, and quality x . Similar to the development of conventional film boiling correlations, these parameters all reflect overall properties of the flow in the pipe and are not directly related to flow regimes. Thus it cannot be used to predict the local heat transfer coefficients in chilldown.

Chen's (ref. 25) flow boiling correlation is based on separating the heat transfer to micro- and macro-convection heat transfer. Micro-convection heat transfer represents the contribution from boiling heat transfer, and macro-convection represents the contribution from the forced convection heat transfer. However his correlation fits best for annular flow because of the derivation of suppression factor. In stratified flow regime, which is common in cryogenic chilldown, Chen's correlation may not be applicable.

Several correlations have been tried in this study, including Gungor and Winterton's correlations (ref. 26), Chen's correlation (ref. 25), and Kutateladze's correlations (ref. 29). None gives a satisfactory heat transfer rate that is need to match the experimentally measured temperature histories in (ref. 7) in the nucleate boiling regime. Among them, Kutateladze's correlation gives more reasonable result. In this correlation, the total heat transfer coefficient h is

$$h = h_{conv} + h_{pool}, \quad (26)$$

where h_{conv} is given by Dittus-Boelter equation for fully developed pipe flow,

$$h_{conv} = 0.023 * Re_l^{0.8} Pr_l^{0.4} * k_l / D \quad (27)$$

and pool nucleated boiling heat transfer coefficient h_{pool} is

$$h_{pool} = 0.487 * 10^{-10} * \left[\frac{k_l \rho_l^{1.282} p^{1.750} (c_{p,l})^{1.5}}{(h_{fg} \rho_v)^{1.5} \sigma^{0.906} \mu_l^{0.626}} \right] \Delta T^{1.5}, \quad (28)$$

in which ΔT is wall superheat.

Kutateladze's correlation (ref. 29) was proposed without considering the effect of nucleate site suppression. This obviously leads to an overestimation of the nucleate boiling heat transfer rate. Hence a modified version of Kutateladze's correlations (28) is used,

$$h = h_{conv} + S * h_{pool}, \quad (29)$$

with S being the suppression factor and h_{pool} is given by (28).

When ΔT drops to a certain range all the nucleate sites are suppressed. The heat transfer is dominated by single phase forced convection. The heat transfer coefficient can then be predicated using Dittus-Boelter equation, eq. (27), if flow is turbulent, or eq. (30), if flow is laminar.

$$h_{conv} = 4.36 * k_l / D . \quad (30)$$

Heat Transfer between Vapor and Solid Wall

The heat transfer between the vapor and the wall can be estimated by treating the flow as a fully developed convection flow, neglecting the liquid droplets that are entrapped in the vapor. The heat transfer coefficient of vapor forced convection flow is

$$h_v = 0.023 * Re_v^{0.8} Pr_v^{0.4} * k_v / D \text{ (turbulent flow)} \quad (31)$$

or

$$h_v = 4.36 * k_v / D \text{ (laminar flow)} \quad (32)$$

Heat Transfer between Solid Wall and Environment

For a cryogenic flow facility, although serious insulation is applied, the heat leakage to environment is still considerable due to the large temperature difference between the cryogenic fluid and the environment. It is necessary to evaluate the heat leakage from the inner pipe to environment in order to make realistic assessment of the model prediction with the experimental results (ref. 7).

Vacuum insulation chamber between the inner and outer pipes is used in cryogenic transport pipe (ref. 7), as shown in figure 5. Radiation heat transfer exists between the inner and outer pipe. Furthermore, the space between the inner and outer pipe is not an absolute vacuum. There is residual air that causes free convection between the inner and outer pipes driven by the temperature difference of the inner and outer pipe.

The radiation between the inner pipe and outer pipe becomes significant when the inner pipe is chilled down. The heat transfer coefficient is proportional to the difference of the fourth power of wall temperatures. Exact evaluation of the radiation heat transfer between the inner and outer pipe is a difficult task. Hence a simplified model based on the overall radiation heat transfer between long concentric cylinders with constant temperature at inner pipe and outer pipe (ref. 31) is used to evaluate the heat transfer rate at every axial location of the pipe. It is not quantitatively correct, but can provide reasonable estimate for the magnitude of the radiation heat transfer between pipes through the vacuum. The local radiation heat transfer rate per unit area on the surface of inner pipe q'_{rad} is

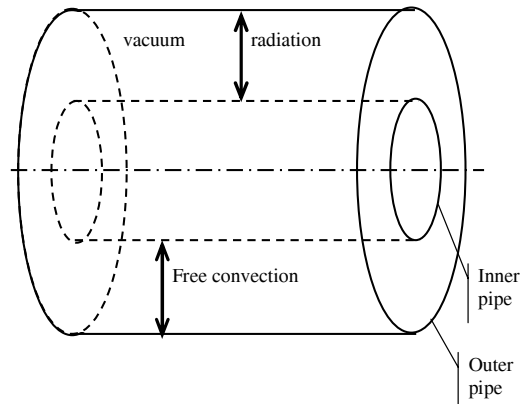


Figure 5.—Schematic of vacuum insulation chamber.

$$q'_{rad} = \frac{\sigma(T_{wall}^4 - T_o^4)}{\frac{1}{\varepsilon_i} + \frac{1 - \varepsilon_o}{\varepsilon_o} \left(\frac{r_i}{r_o} \right)}, \quad (33)$$

where the σ is Stefan Boltzmann constant, (r_i, ε_i) and (r_o, ε_o) are the radius and emissivity of inner pipe and outer pipe, respectively, and T_{wall} is the local inner wall temperature, T_o is the room temperature that is assumed constant in the entire outer pipe. Here the emissivity is also assumed to be constant during the entire chilldown process.

For the free convection heat transfer due to the residual air in the vacuum chamber between the inner pipe and outer pipe, Raithby and Hollands' correlation (ref. 35) is used for the heat transfer rate. The average heat transfer rate per unit length of the cylinder is

$$q'_{frc} = \frac{2\pi k_{eff}}{\ln\left(\frac{r_o}{r_i}\right)} (T_i - T_o), \quad (34)$$

where T is assumed constant on the inner and outer wall along the azimuthal directions, and k_{eff} is the effective thermal conductivity.

Results and Discussions

In experiment by Chung et al. (ref. 7), liquid nitrogen was used. The flow regime is revealed to be stratified flow by visual observation, as shown in figure 7, and wall temperature history in several azimuthal positions is measured by thermal couples and recorded on a computer.

Experiment of Chung et al.

In experiment of Chung et al. (ref. 7), a concentric pipe test section (fig. 6) was used. The chamber between the inner and outer pipe is vacuumed, but about 20 percent air remained. The inner diameter (i.d.) and outer diameter (o.d.) of inner pipe are 11.1 and 15.9 mm, and i.d. and o.d. of outer pipe are 95.3 and 101.6 mm, respectively. Numerous thermal couples were placed at different locations of the inner pipe. Some were embedded very closely to the inner surface of the inner pipe while others measure the outside wall temperature of inner pipe. Experiments were carried out at room temperature and atmosphere pressure. Liquid nitrogen flows from a reservoir to the test section driven by gravity. As liquid nitrogen flows through the pipe, it evaporates and chills the pipe. Some of the typical visual results are shown in figure 7. The measured average liquid nitrogen velocity is $U \sim 5$ cm/s. Vapor velocity is not measured in this experiment. In this study, it is determined through trial-and-error by fitting the computed and measured temperature histories. The characteristic liquid volume fraction is 0.3 from the recorded video images. The characteristic time used in this computation is $t_0 = 100$ s. The Leidenfrost temperature for the nitrogen is around 180 K; hence the temperature when the film boiling ends and nucleates boiling starts is set at 180 K. The transition temperature at which the nucleate flow boiling switches to purely convection heat transfer is 140 K based on experimental results. The material of the inner pipe and outer pipe used in the experiment of (ref. 7) are Pyrex glass with emissivity of 0.82 at room temperature.

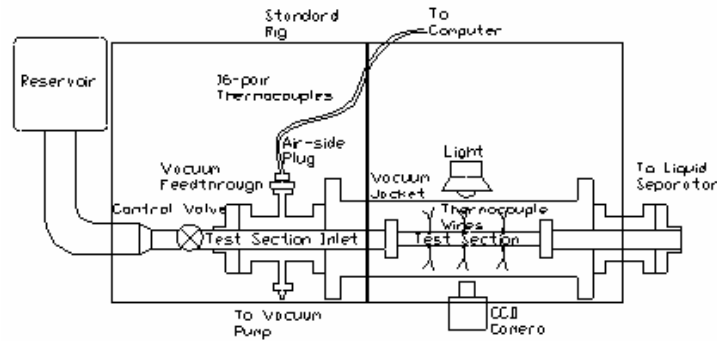


Figure 6.—Schematic of Chung et al.'s cryogenic two-phase flow test apparatus (ref. 7).

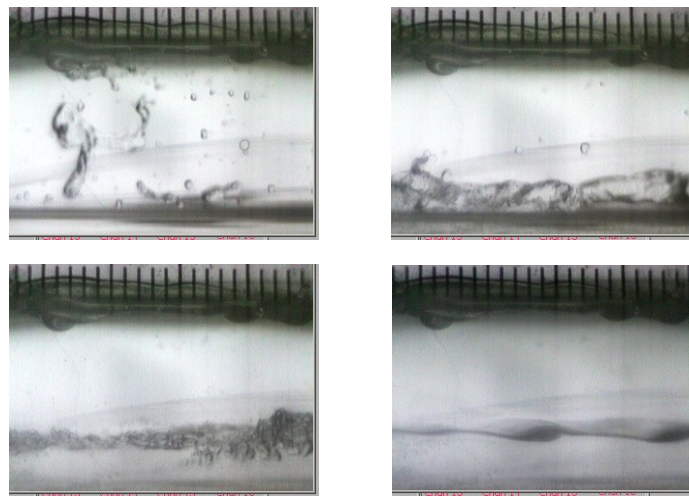


Figure 7.—Experimental visual observation of Chung et al.'s cryogenic two-phase flow test (ref. 7).

Comparison of Pipe Wall Temperature

In the computation, there are 40 grids along the radial direction and 40 grids along azimuthal direction for the inner pipe (fig. 8). The results of temperature profile at 40×40 grids and higher grids resolution show that 40×40 grids are sufficient. Figures 9 and 10 compare the measured and computed wall temperature as a function of time at positions 11, 12, 14 and 15 shown in figure 8. For the modified Kutateladze's correlation a suppression factor 0.01 is used. Vapor velocity is 0.5m/s based on the best fit. The overall temperature histories agree well in the film boiling stage. Thus, the film boiling heat transfer coefficient based on the first principle and incorporated the flow structure gives very reliable prediction. It must also be noted that the value of the Leidenfrost temperature does not affect the computed temperature history prior to that transition point since the governing equation is parabolic. The good agreement before the Leidenfrost temperature is reached is entirely due to the superior performance of the new film boiling heat transfer coefficient.

During the stage of the rapidly decreasing wall temperature after the Leidenfrost temperature, the computed wall temperature drops slightly faster than the measured value. The rapid decrease in the wall temperature is due to initiation of nucleate boiling which is more efficient for heat transfer than the film boiling. Reasonable agreement between the computed and measured histories in this nucleate boiling regime is due to: i) the good agreement already achieved in the film boiling stage; ii) valid choice for the Leidenfrost temperature that switches the heat transfer regime correctly; and iii) appropriate modification of Kutateladze's correlations.

In the final stage of cooldown, the wall temperature decreases slowly, and the computed wall temperature shows the same trend as the measured one but tends to be a little lower. Figure 11 shows the temperature distribution of a given cross-section at different times of cooldown. Because the upper part of pipe wall is exposed to nitrogen vapor, cooling effect is much reduced.

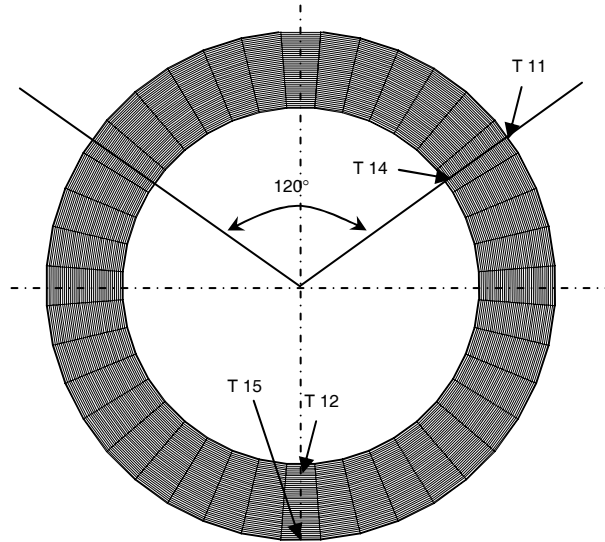


Figure 8.—The computational grids arrangement and positions of thermal couples.

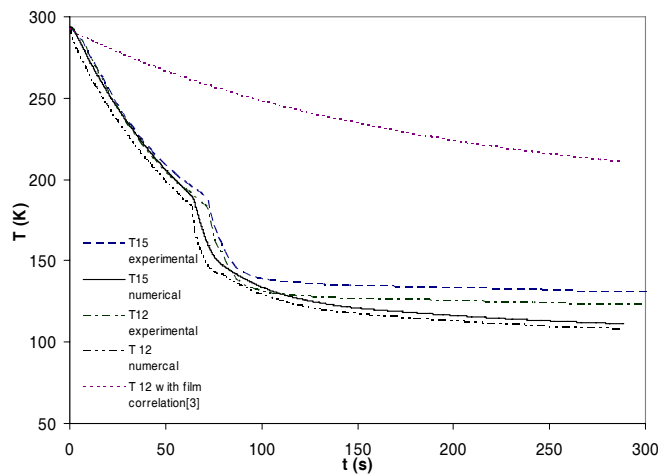


Figure 9.—Comparison of wall temperature of transducer 12 and 15, which is at the bottom of pipe, between the experiment and computation. For comparison purpose, the solution in the Z-direction is converted to time t .

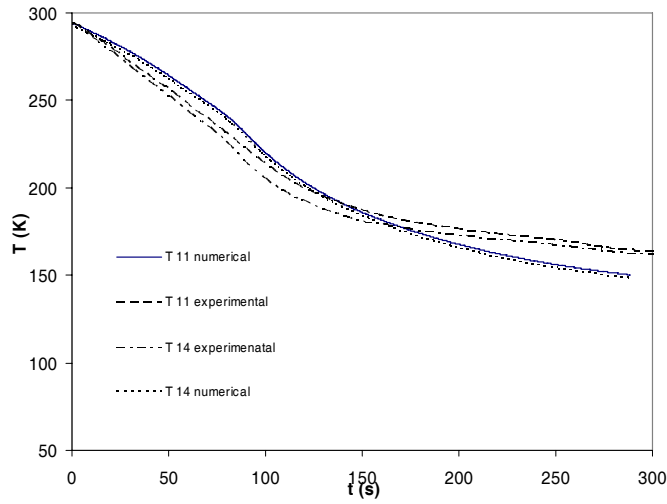


Figure 10.—Comparison of wall temperature of transducer 11 and 14, which are at the upper part of the pipe, between the experiment and computation. For comparison purpose, the solution in the Z -direction is converted to time t .

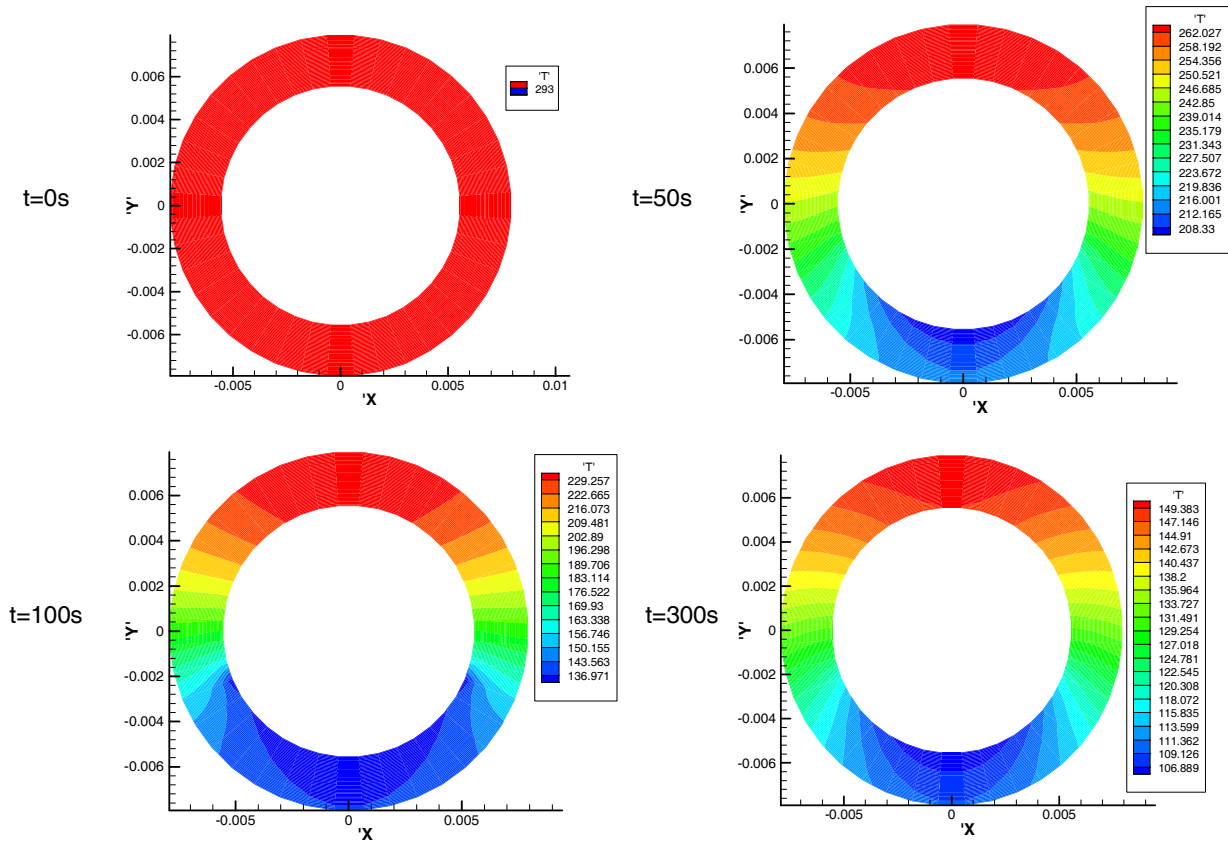


Figure 11.—Wall temperature distribution across the section at $t = 0, 50, 100$ and 300 sec.

Discussions and Remarks

In figure 9, the wall temperature based on the film boiling correlation of Giarratano and Smith (ref. 24) is also shown. Apparently, the correlation of Giarratano and Smith (ref. 24) gives a very low heat transfer rate so that the wall temperature remains high. This comparison confirms our earlier argument that correlations based on the overall flow parameter, such as quality and averaged Reynolds number, are not applicable for the simulation of unsteady chilldown.

The nucleate flow boiling correlations of Gungor and Winterton (ref. 26), Chen (ref. 25), Kutateladze's correlations (ref. 29) are also compared in this study. Gungor and Winterton's correlation fails to give a converged heat transfer rate during the transition from the film boiling to the nucleate boiling. Chen's correlation overestimates the heat transfer rate, and cause unrealistically large temperature drop on the wall, which results in the halt of the computation. Only Kutateladze's correlation gives a reasonable heat transfer rate. However, the temperature drop near the bottom of the pipe is still faster than the measured one as shown in figure 9. This may be due to the fact that most of nucleate boiling correlations were obtained from experiments of low wall superheat. However, in this cryogenic chilldown, wall superheat is much higher than that in the normal nucleate boiling experiments. Another reason is that the original Kutateladze's correlation does not include suppression factor. This leads to overestimating heat transfer coefficient. The modified Kutateladze's correlation with suppression factor gives reasonable chilldown result in figure 9.

Further examination of figures 9 and 10 indicates that although we have considered the heat leak from the outer wall to the inner wall through radiation and free convection, the computed temperature is still lower than the measured temperature during the final stage of chilldown, where the heat transfer rate between fluid and wall is low due to lower wall superheat and possibly heat leak. The temperature difference between the computed and measured values at position 12 and position 15 suggests that there may be additional heat leak, which affects the measurements but is not taken in account in the present modeling.

In this study, the pseudo-steady chilldown model is developed to predict the chilldown process in a horizontal pipe in stratified flow regime. This model can also be extended to describe annular flow chilldown in the horizontal or the vertical pipe with minor changes on the boundary condition for solid temperature. It can also be extended to study the chilldown in the slug flow as long as we specify the contact period between the solid and the liquid or the vapor. The disadvantage of the current pseudo-steady chilldown model is that the fluid interaction inside the pipe is largely neglected and both vapor and liquid velocities are assumed to be constant. Compared with a more complete model that incorporates the two-fluid model, the present pseudo-steady chilldown model requires more experimental measurements as inputs. However, the pseudo-steady chilldown model is computationally more robust and efficient for predicting chilldown process. It provides overall reasonable results for the solid wall temperature. While a more complete model for chilldown process that incorporates the mass, momentum, and energy equations of vapor and liquid is being developed to reduce the dependence of the experimental inputs for the liquid velocity and trial-and-error for the vapor velocity, the present study has revealed useful insights into the key elements of two-phase heat transfer encountered in the chilldown process which have been largely ignored. It also laid the necessary modeling foundation for the incorporation of the two-fluid model.

Conclusions

A pseudo-steady chilldown computational model has been developed to understand the heat transfer mechanisms of cryogenic chilldown and predict the chilldown wall temperature history in a horizontal pipeline. The model assumes the constant speed of the moving liquid wave front, and steady state of the thermal field in the solid in a reference frame that moves with the liquid wave front, and saturated temperature of both liquid and vapor so that the 3-D unsteady problem can be transformed to a 2-D, parabolic problem. A new film boiling heat transfer coefficient in the cryogenic chilldown condition is developed using the first principle and incorporating the stratified flow structure. The existing nucleate

boiling heat transfer correlations may not work well under cryogenic condition. A modified Kutateladze's correlations with suppression factor adequately describes heat transfer coefficient. With the new and modified heat transfer correlations, the pipe wall temperature history based on the pseudo-steady chilldown model matches well with the experimental results by Chung et al. (ref. 7) for almost the entire chilldown process. The pseudo-steady chilldown model has captured the important features of thermal interaction between the pipe wall and the cryogenic fluid.

References

1. Burke, J.C., Byrnes, W.R., Post, A.H., and Ruccia, F.E., 1960, "Pressure Cooldown of Cryogenic Transfer Lines," *Advances in Cryogenic Engineering*, **4**, pp. 378–394.
2. Graham, R.W., Hendricks, R.C., Hsu, Y.Y., and Friedman, R., 1961, "Experimental Heat Transfer and Pressure Drop of Film Boiling Liquid Hydrogen Flowing through A Heated Tube," *Advances in Cryogenic Engineering*, **6**, pp. 517–524.
3. Bronson, J.C., Edeskuty, F.J., Fretwell, J.H., Hammel, E.F., Keller, W.E., Meier, K.L., Schuch, and A.F, Willis, W.L., 1962, "Problems in Cool-Down of Cryogenic Systems," *Advances in Cryogenic Engineering*, **7**, pp. 198–205.
4. Chi, J.W.H., and Vetere, A.M., 1963, "Two-Phase Flow During Transient Boiling of Hydrogen and Determination of Nonequilibrium Vapor Fractions," *Advances in Cryogenic Engineering*, **9**, pp. 243–253.
5. Steward, W.G., Smith and R.V., Brennan, J.A., 1970, "Cooldown Transients in Cryogenic Transfer Lines," *Advances in Cryogenic Engineering*, **15**, pp. 354–363.
6. Velat, C., Jackson, J., Klausner, J.F., and Mei, R., 2004, "Cryogenic Two-Phase Flow during Chilldown," in *Proceedings of the ASME HT-FED Conference*, Charlotte, NC.
7. Chung, J.N., Yuan, K., and Xiong, R., 2004, "Two-Phase Flow and Heat Transfer of a Cryogenic Fluid during Pipe Chilldown," *Proceedings of 5th International Conference on Multiphase Flow*, Yokohama, Japan, pp. 468.
8. Martinelli, R.C., and Nelson, D.B., 1948, "Prediction of Pressure Drop During Forced –Circulation Boiling of Water," *Transaction of ASME*, **70**, pp. 695–701.
9. Chi, J.W.H., 1965, "Cooldown Temperatures and Cooldown Time During Mist Flow," *Advances in Cryogenic Engineering*, **10**, pp. 330–340.
10. Cross, M.F., Majumdar, A.K., Bennett Jr., and J.C., Malla, R. B., 2002, "Model of chilldown in Cryogenic Transfer Linear," *Journal of Spacecraft and Rockets*, **39**, pp. 284–289.
11. Chan, A.M.C., and Banerjee, S., 1981, "Refilling and Rewetting of a Hot Horizontal Tube part I: Experiment," *Journal of Heat Transfer*, **103**, pp. 281–286.
12. Chan, A.M.C., and Banerjee, S., 1981, "Refilling and Rewetting of a Hot Horizontal Tube part II: Structure of a Two-Fluid Model," *Journal of Heat Transfer*, **103**, pp. 287–292.
13. Chan, A.M.C., and Banerjee, S., 1981, "Refilling and Rewetting of a Hot Horizontal Tube part III: Application of a Two-Fluid Model to Analyze Rewetting," *Journal of Heat Transfer*, **103**, pp. 653–659.
14. Bromley, J.A., 1950, "Heat Transfer in Stable Film Boiling," *Chemical Engineering Progress*, **46**, no. 5, pp. 221–227.
15. Dougall, R.S., Rohsenow, W.M., 1963, "Film boiling on the inside of vertical tubes with upward flow of the fluid at low qualities," MIT report no 9079–26, MIT.
16. Lavery, W.F., and Rohsenow, W.M., 1967, "Film Boiling of saturated Nitrogen Flowing in a Vertical Tube," *Journal of Heat transfer*, **89**, pp. 90–98.
17. Bromley, J.A., 1950, "Heat Transfer in Stable Film Boiling," *Chemical Engineering Progress*, **46**, no. 5, pp. 221–227.
18. Breen, B.P., and Westwater, J.W., 1962, "Effect if Diameter of Horizontal Tubes on Film Heat Transfer," *Chemical Engineering Progress*, **58**, no.7, pp. 67.

19. Berenson, P.J., 1961, "Film-Boiling Heat Transfer from a Horizontal Surface," *Journal of Heat Transfer*, **83**, pp. 351–358.
20. Hendricks, R.C., Graham, R.W., Hsu, Y.Y., and Friedman, R., 1961, "Experimental Heat Transfer and Pressure Drop of Liquid Hydrogen Flowing Through a Heated Tube," NASA TN D-765.
21. Hendricks, R.C., Graham, R.W., Hsu, Y.Y., and Friedman, R., 1966, "Experimental Heat Transfer Results for Cryogenic Hydrogen Flowing in Tubes at Subcritical and Supercritical Pressure to 800 pounds per Square Inch Absolute," NASA TN D-3095.
22. Ellerbrock, H.H., Livingood, J.N.B., and Straight, D.M., 1962, "Fluid-Flow and Heat-Transfer Problems in Nuclear Rockets," NASA SP-20.
23. von Glahn, U.H., 1964, "A Correlation of Film-Boiling Heat Transfer Coefficients Obtained with Hydrogen," Nitrogen and Freon 113 in Forced Flow, NASA TN D-2294.
24. Giarratano, P.J., Smith, R. V., 1965, "Comparative study of Forced Convection Boiling Heat Transfer Correlations for Cryogenic Fluids," *Advances in Cryogenic Engineering*, **11**, pp. 492–505.
25. Chen, J.C., 1966, "Correlation for Boiling Heat Transfer to Saturated Fluids in Convective Flow," *Industry Engineering Chemistry Process Design and Development*, **5**, pp. 322–329.
26. Gungor, K.E., Winterton, R.H.S., 1996, "A General Correlation for Flow Boiling in Tubes and Annuli," *International Journal of Heat Mass Transfer*, **29**, No.3, pp. 351–358.
27. Bennett, D.L., and Chen, J.C., 1980, "Forced Convection for the in Vertical Tubes for Saturated Pure Components and Binary Mixture," *A.I.Ch.E. Journal*, **26**, pp. 454–461.
28. Stephan, K., and Auracher, H., 1981, "Correlation for Nucleate Boling Heat Transfer in Forced convection," *International Journal of Heat Mass Transfer*, **24**, pp.99–107.
29. Kutateladze, S.S., 1952, "Heat Transfer in Condensation and Boiling," Atomic Energy Commission Translation 3770, Tech. Info. Service, Oak Ridge, Tennessee.
30. Steiner, D., May 1986, "Heat Transfer During Flow Boiling of Cryogenic Fluids in Vertical and Horizontal Tubes," *Cryogenics*, **26**, pp. 309–318.
31. Incropera, F.P., Dewitt, D.P., 2002, *Fundamentals of Heat and Mass Transfer*, 5th edition, John Willey& Sons.
32. Thompson, T.S., 1972, "An Analysis of the Wet-Side Heat-Transfer Coefficient during Rewetting of a Hot Dry Patch," *Nuclear Engineering and Design*, **22**, pp. 212–224.
33. Ferderking, T.H.K., and Clark, J.A., 1963, "Nature Convection Film Boling on A Sphere," *Advanced Cryogenic Engineering*, **8**, pp. 501–506.
34. Carey, V.P., 1992, *Liquid-Vapor Phase-Change Phenomena*, Taylor & Francis Press.
35. Raithby, G.D., and Hollands, K.G.T., 1975, "A General Method of Obtaining Approximate Solutions to Laminar and Turbulent Free Convection Problems," *Advances in Heat Transfer*, **11**, pp.265–315 Academic Press, New York.